Bone Response Inside Free-Form Fabricated Macroporous Hydroxyapatite Scaffolds with and without an Open Microporosity

Johan Malmström, DDS;* Erik Adolfsson, MSc, PhD;† Anna Arvidsson, MSc, PhD;*
Peter Thomsen, MD, PhD*

ABSTRACT

Background: The technique of free-form fabrication enables the production of controlled macroporous geometry inside ceramic scaffolds. Using scaffolds with identical macropore design makes it possible to study a relevant biological response linked to other specific changes of the material.

Purpose: This study investigates the role of open micropores in hydroxyapatite (HA) scaffold during early bone healing to quantitatively ascertain whether microporosity in otherwise identical macroporous HA scaffolds can influence the bone response in rabbit tibia and femur at 6 weeks.

Materials and Methods: HA scaffolds (Ø: 3.8 mm) with and without microporosity were randomly installed in both cortical and trabecular bone sites of New Zealand White rabbits. The animals were sacrificed 6 weeks after surgery. Ground sections obtained from en bloc tissues containing scaffold and recipient bone were subjected to histological evaluation and histomorphometric analysis.

Results: Microscopy showed elevated amounts of bone ingrowth and bone contact inside the microporous HA (mHA) group as compared with non-mHA.

Conclusion: The current study indicates that the presence of open scaffold microporosity in HA, as determined by the fabrication process, enhances the ability of ceramic scaffolds to promote bone ingrowth and bone contact.

KEY WORDS: bone regeneration, free-form fabrication, hydroxyapatite, macroporosity, microporosity, scaffolds

Porous ceramics have been considered for use as bone graft substitutes in the treatment of bone defect for over 30 years.[1] Calcium phosphates are ceramics that show a highly attractive biologic profile. The underlying basis for the lack of local or systemic toxicity with calcium phosphates is their chemical nature, as they contain mainly calcium and phosphate ions.[2,3] Hydroxyapatite (HA) is one of the most commonly used calcium phosphates to be used as a bone substitute in orthopedic, dental, and maxillofacial surgery.[4] To promote bone ingrowth in ceramic scaffolds, different geometries of the pore system have been evaluated.[5] The relationship between pore dimension and tissue ingrowth in HA has been evaluated and there is a positive correlation between these parameters. The larger the macropores, the more is the tissue ingrowth if the pore diameter is greater than 150 µm.[6–9] Micropore geometries are often present in HA samples as they result from incomplete densification of the HA particles during processing.[10]

The microporosity variations tested in various ceramic/tissue studies have usually been created by altering the sintering process[11,12] or the shaping process.[13] When the sintering temperature is changed in order to vary the microporosity in ceramic materials, other material characteristics such as grain size will be changed. For

*Institute for Clinical Sciences, Department of Biomaterials, Göteborg University, Sweden; †Swedish Ceramic Institute, IVF, Mölndal, Sweden

Reprint requests: Johan Malmström, Department of Biomaterials, Box 412, 405 30, Göteborg, Sweden; e-mail: johan.malmstrom@biomaterials.gu.se

DOI 10.1111/j.1708-8208.2007.00031.x

calcium phosphate materials, the temperature change can also influence both phase and chemical composition of the prepared material. This indicates that temperature is a less suitable parameter to use when the biological response to microporosity is to be studied. An open microporosity establishes connections between macropores.[9] These micropores allow circulation of interstitial fluid through them, which in turn are believed to facilitate blood vessel and tissue ingrowth into the HA.[14] Today, however, there is little and contradictory information regarding the influence of microporosity on bone formation.[5,13] Recent in vitro and in vivo studies have demonstrated bone cell sensitivity to the level of microporosity within the ceramic strut,[15,16] and there are indications that manipulation of the levels of microporosity within HA scaffolds can be used to accelerate osseointegration.[5] On the other hand, results have also demonstrated no differences in bone response to HA with different levels of microporosity.[13]

The aim of this study was to evaluate the influence of microporosity on early bone formation in scaffold with identical macroporosity.

MATERIALS AND METHODS

Materials

A computer-aided design (CAD) tool (SolidWorks, Concord, MA, USA) was used to design models of scaffolds with square-shaped and interconnected pore channels (Figure 1). Molds corresponding to the designed macroporosities were built with a free-form fabrication (FFF) equipment (Model Maker II®, Sanders, Merrimack, NH, USA) using an inkjet printing principle with a layer thickness of approximately 50 μm. A thermoplastic building material (ProtoBuild™, Sanders) was used for the mold structure, surrounded by a supporting wax-based material (ProtoSupport™, Sanders), allowing overhangs to be built. The support material was separately removed from the mold, leaving a structure of build material corresponding to the macroporosity of the scaffold designed with the CAD tool. The free-form fabricated molds were infiltrated with ceramic suspensions prepared by ball milling of HA (Plasma Biotal, Tideswell, Buxton, UK) with a solids loading of 48 vol%. The microporosity was obtained by an addition of a binder (LDM7651S, Clariant, Muttenz, Switzerland) to the suspension. The ceramic suspensions with and without binder were consolidated using slip casting (colloidal filtration) where the excess of water was drained from the suspension on a plate of plaster. The cast materials were heated with a low heating rate of 1°C/min up to 600°C to burn away the mold and organic additives, and 5°C/min up to 1200°C. The sintering temperature was kept for 2 hours before the temperature was decreased by 5°C/min. The bulk porosity of the sintered materials was measured by Archimedes' principle, and the macroporosity of the scaffold was calculated from the geometrical dimensions of the macroporous structures. The sintered materials were characterized by their x-ray diffraction (XRD) patterns obtained in a Guinier-Hägg camera, using CuKα_1 radiation.

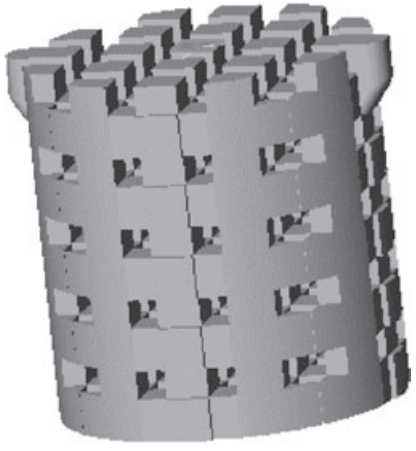

Figure 1 Computer-aided design illustration of scaffold.

Surface Topography

The surface of the sintered materials was studied by scanning electron microscopy (SEM) and optical interferometry (MicroXAM™, PhaseShift, Tucson, AZ, USA). The interferometry analysis was performed with a 50× objective and a zoom factor of 0.625, resulting in a measurement area of $200 \times 260\,\mu m^2$. In total, three specimens of each type of material were used for the topographical characterization. Interferometer measurements were made on two beam surfaces of each material representing the inside of the macropores created by the manufacturing process, referred to as: (P), side parallel to manufacturing direction, and (O), side orthogonal to manufacturing direction (Figure 2). The topography of (P) and (O) sides was described as the mean of 30 measurements for each surface and material resulting in two surface roughness values for each scaffold material. The errors of form were removed with a $50 \times 50\,\mu m^2$ digital Gaussian filter before calculating the

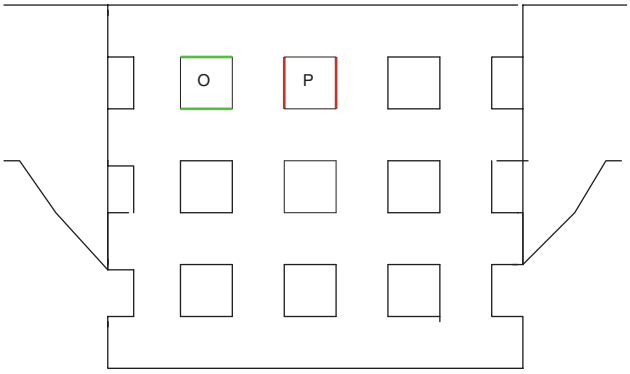

Figure 2 Schematic picture demonstrating side parallel to manufacturing direction (P) and side orthogonal to manufacturing direction (O) inside macropore representing different surface roughness values.

following topographical parameters: (1) the average height of structures from a mean plane (S_a), (2) the number of peaks per unit area (S_{ds}), (3) the developed surface ratio (S_{dr}), (4) texture aspect ratio used to separate isotropy and anisotropy of surfaces (S_{tr}), and (5) the core fluid retention index (S_{ci}). The (P) sides had a higher surface roughness than the (O) sides, irrespective of material. For non-microporous HA (mHA), a surface enlargement was seen for the (P) side compared to the (O) side, as characterized by S_{dr}. In the mHA, a clear orientation could be seen for the (P) side compared to the (O) side, as characterized by S_{tr} (Table 1). The evaluation regarding bone contact was performed by comparing the two different surfaces (P, O) in the macropores for each material.

Animals and Anesthesia

Nine adult female New Zealand White rabbits weighing 4.7 to 5.8 kg and fed ad libitum were used in the study. Prior to surgery, the animals were anesthetized by intramuscular injections of a combination of phentanyl and fluanizon (Hypnorm®, Janssen, Brussels, Belgium; 0.7 mg/kg body weight [b.wt.]), and intraperitoneal injection of diazepam (Stesolid®, Dumex, Copenhagen, Denmark; 1.5 mg/kg b.wt.). Lidocaine (5% Xylocain®, Astra AB, Södertälje, Sweden) was infiltrated subcutaneously to obtain local anesthesia. The animals were given trimetoprim 40 mg + sulfadoxin 200 mg/mL (Borgal® vet, Hoechst AB) prior to surgery and 2 days postoperatively. Analgetics, buprenorphine (Temgesic®, Schering-Plough, Stockholm, Sweden; 0.3 mg/mL), were given during 3 days postoperatively. Fluorochrome markers for bone formation were given as single injections to the animals at two occasions. Oxytetracycline (Sigma, St. Louis, MO, USA) was given at a dose of 25 mg/kg b.wt. 4 weeks postoperatively. Alizarin complexone (Sigma) was given at a dose of 30 mg/kg b.wt. 5 weeks postoperatively.

Surgery

According to a randomized implant insertion scheme, 36 implants (18 of each type) were placed in nine adult female New Zealand White rabbits. The experiment was approved by the Local Ethics Committee, Göteborg University. The limbs were shaved and disinfected with chlorhexidine (5 mg/mL, Pharmacia AB, Stockholm, Sweden). The operations were performed under sterile

TABLE 1 Topographical Results Representing Side Parallel to Manufacturing Direction (P) and Side Orthogonal to Manufacturing Direction (O) Inside Macropores as Measured with Optical Interferometry Measurements

Specimen Type	Side	*n*	S_a (μm)	S_{ds} (μm^{-2})	S_{dr} (%)	S_{tr}	S_{ci}
Non-mHA	P	30	2.54	0.105	200.66	0.46	1.40
			(0.63)	(0.008)	(69.88)	(0.16)	(0.20)
	O	30	0.44	0.128	16.72	0.24	1.24
			(0.10)	(0.016)	(5.35)	(0.18)	(0.11)
mHA	P	30	2.40	0.103	95.80	0.42	1.52
			(0.41)	(0.003)	(21.92)	(0.25)	(0.09)
	O	30	1.70	0.101	79.87	0.66	1.44
			(0.33)	(0.005)	(18.72)	(0.08)	(0.09)

The figures represent means, standard deviations within parentheses.

conditions. Each animal received two implants of the same type in one leg and two implants of other type in the contralateral leg. One implant was inserted in each proximal tibial metaphysis and one implant in each medial femoral condyle according to a random scheme. The implant areas were exposed separately through skin incisions and blunt dissection of the underlying tissue, including the periosteum. The holes in both the tibia and femur were made using dental implantation drills up to a diameter of 3.8 mm under profuse irrigation with sterile saline (NaCl 9 mg/mL, ACO Läkemedel AB, Solna, Sweden). The scaffolds were then gently pressed in the defects. The operation site was rinsed with saline and the tissues were sutured in separate layers with Vicryl® 5-0 (Ethicon, Norderstedt, Germany) and finally intracutaneous with Monovicryl® 4-0 (Ethicon).

Animal Sacrifice and Ground Sectioning

The animals were sacrificed after 6 weeks with an overdose of barbiturate (Mebumal®, ACO Läkemedel AB) and fixed by perfusion via the left heart ventricle with 2.5% glutaraldehyde in 0.05 M sodium cacodylate buffer, pH 7.4. The scaffolds and the surrounding bone were removed en bloc, further immersed in glutaraldehyde for 2 to 4 days. After dehydration in ethanol, the undecalcified specimens were embedded in plastic resin (LR White™, the London Resin Co. Ltd, Hampshire, UK). The specimens were divided longitudinally by sawing (Exact cutting and grinding equipment, Exact Apparatebau, Norderstedt, Germany), and ground sections (thickness: 15–20 µm) were prepared and stained with 1% toluidine blue.[17,18]

Microscopy and Morphometry

Light microscopic (LM) morphometry and fluorochrome analysis were performed on the ground sections using an Eclipse E600™ (Kawasaki, Kanagawa, Japan) light microscope and connected computer software.

SEM

The HA (with and without microporosity) was examined using SEM. A high-resolution Leo 1550 FEGSEM was used for the analysis.

Statistical Analysis

The Wilcoxon signed rank sum test was used for statistical analysis. A p value of $<.05$ was set for significance.

TABLE 2 Results Representing Open, Closed, and Total (vol.%) of Microporosity in Dense and Microporous Hydroxyapatite

Microporosity	Open (vol%)	Closed (vol%)	Total (vol%)
Dense	0	0.8	0.8
Micro	22.1	0.2	22.3

RESULTS

Materials

The size of the free-form fabricated molds was rescaled individually for each material to be cast in order to compensate for the different shrinkages during densification. The fabricated scaffolds had an identical macroporosity, consisting of square-shaped and interconnected pore channels with a size around 350 microns and a macroporosity around 40 vol%. When the cast material of HA without binder was sintered at 1200°C, an almost fully dense material was obtained (Table 2). The remaining porosity consisted of small closed pores, which would not influence the biological response. With an addition of binder to the ceramic suspension, the sintered density was around 78% when sintered at 1200°C. The remaining microporosity was sufficient to obtain a continuous microporosity that was interconnected to around 99%. Apatite was the only phase detected from the XRD analysis of the HA powder used. After densification, a trace of tricalcium phosphate was also detected because of a minor Ca deficiency of the powder (Figure 3).

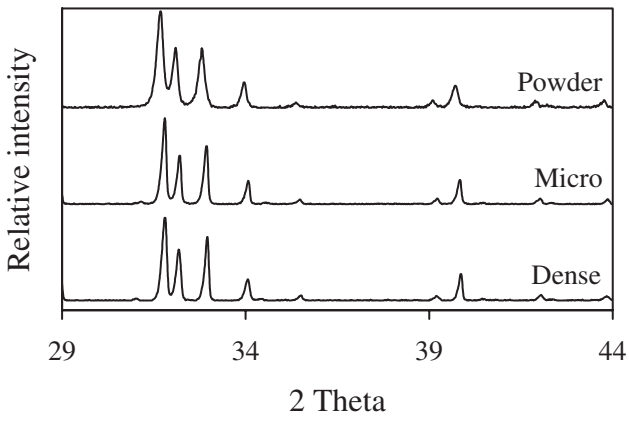

Figure 3 X-ray diffraction patterns from the powder and sintered materials (dense and microporous).

Histologic Analysis

The scaffolds were well integrated in both cortical and trabecular bone 6 weeks after insertion. Light microscopy of the bone adjacent to scaffolds showed remodeling – most evident in tibial cortical bone (Figure 4, A and D). The newly formed bone (NB) could be distinguished from the mature bone (see Figure 4A). A distinct border between bone and scaffold was evident. Bone trabeculae were observed extending from the endosteum/periosteum as well as from the cut bone surface toward the scaffold (Figure 5A). Blood vessels were detected inside the NB irrespective of scaffold type and bone beds. The tissue response for both materials consisted mainly of NB filling the scaffolds. The fluorochrome labeling demonstrated that the bone was woven and that the bone had started to form and remodel at 4 weeks inside the scaffolds (Figure 6, A–D). No signs of inflammatory reactions could be detected in the tissues surrounding the implants.

SEM

Morphological differences could be seen analyzing both materials with SEM (Figures 7 and 8). The interconnected open microporosity of the material was estimated from SEM to have a size around a few microns (see Figure 7).

Quantitative Analysis

The morphometric analysis consisted of: (1) determination of the amount of bone within the scaffold, expressed as percent bone area and (2) determination of the degree of bone-scaffold contact inside the scaffold, expressed as percent bone contact. No significant differences in the bone area parameters were detected between the two materials, irrespective of implantation site (Figure 9). A significant higher bone contact was observed for mHA in comparison with non-mHA (Figure 10). There were no significant differences in bone contact, irrespective of material, between the different surfaces (P and O) inside the macropores (data not shown).

DISCUSSION

The technology of FFF offers a rational production of small lots as well as customization of designs, providing important research tools. The ability to directly build complex geometries also makes CAD to ceramic technology interesting for future manufacturing of fully functional customized scaffolds. Features of macroporosity, such as volume fraction, pore size, and pore connectivity, are recognized to affect and to be of importance for the final volume of regenerated bone.[11,12,19–22] In the present study, using HA with identical macroporosity, the presence of 20% open microporosity resulted in the promotion of a significant greater bone contact inside the mHA scaffolds compared to non-mHA at 6 weeks. The promotion of a larger bone contact of mHA was revealed in both cancellous and cortical bone. In addition, the mHA had a greater, albeit not statistically significant, bone ingrowth as measured by LM histomorphometry. No qualitative morphological differences in the bone were seen at the HA–bone interface at the LM level with or without open microporosity in the material. In agreement with this result, Rosa and colleagues[13] showed that there were no morphological differences at the HA–bone interface with respect to the percentage of micropores on the HA surface. The present study also showed that different surface topographies inside the macropores did not change the degree of bone contact. This is in agreement with earlier results using non-mHA and zirconia scaffolds in rabbits.[23] Similar results have also been shown by Sennerby and colleagues[24] comparing zirconia dental screws with different surface topographies. A possible mechanism of action by adding microporosity to ceramic materials has been suggested by Hing and colleagues.[5] The mechanism could be attributed to either increased permeability within the microporous scaffolds enhancing nutrient transfer, leading to faster bone apposition and/or angiogenesis, or it may result from a larger surface area or a geometrically more suitable substrate for angiogenic and/or osteogenic protein adsorption and cell anchorage, leading to a more rapid induction of angiogenesis and bone apposition. A larger surface area provided by the microporosities would also result in larger amounts of dissolved Ca^{2+} and PO_4^{3-} from the scaffold. This might promote the formation of a carbonate HA layer on the surface, and in turn, enhance bone formation according to the hypothesis presented by LeGeros.[25] Whether the introduction of microporosity is inductive or not on bone formation has been tested by Habibovic and colleagues[12] who postulated that the introduction of microporosity within HA implanted in muscle affected the interface dynamics of the ceramic in such a way that relevant cells were triggered to

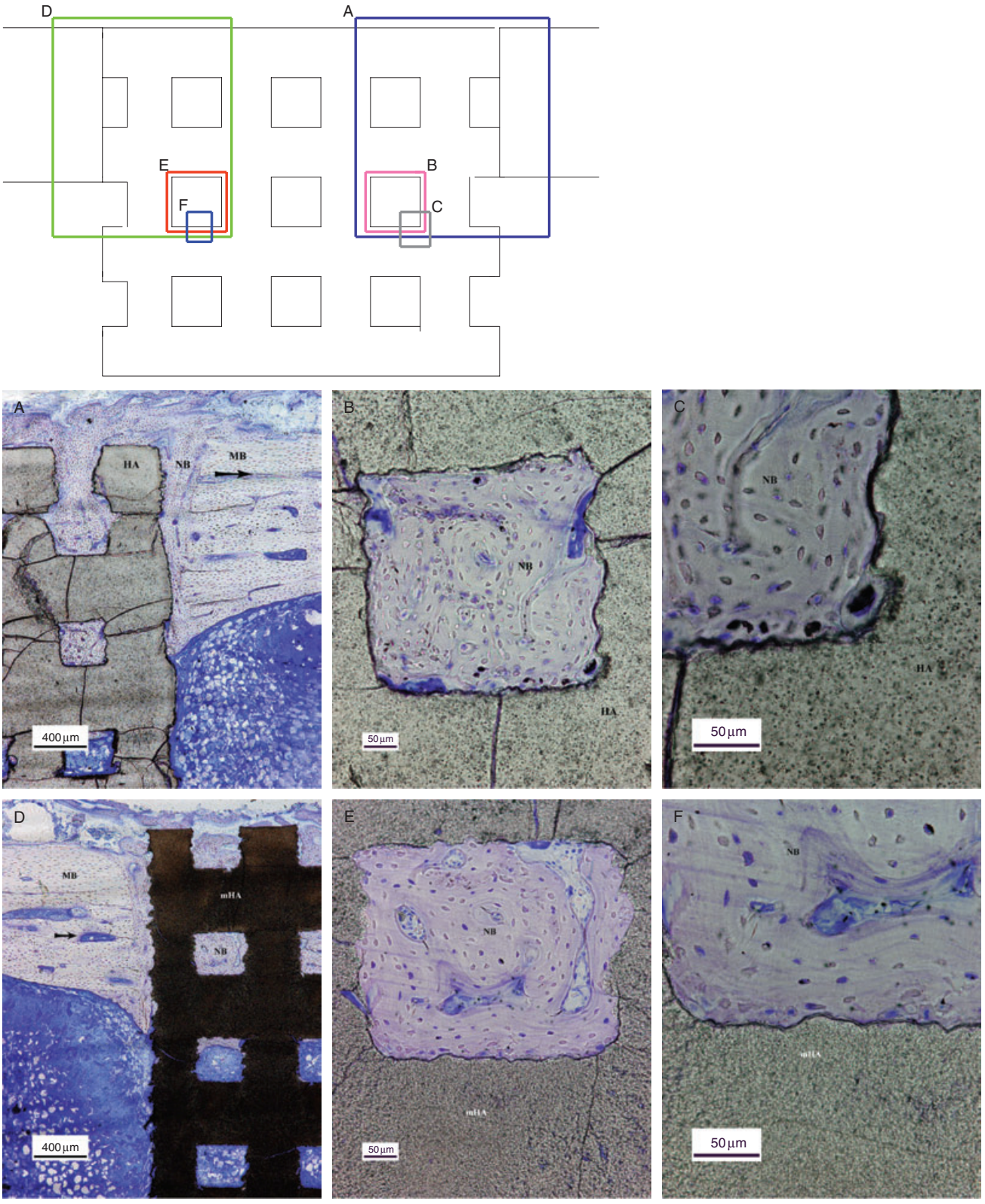

Figure 4A–F Mount of light micrographs (ground sections) of scaffolds in tibia located according to schematic picture (insert, top). *A,* Non-microporous hydroxyapatite (mHA), 6 weeks. Defect border where arrow denotes bone remodeling in mature bone (MB). Newly formed bone (NB) has established contact with the outer surface of the scaffold and the inner surface of the macropore. Bar = 400 µm. *B,* Non-mHA, 6 weeks. Macropore inside scaffold filled with NB. Bar = 50 µm. *C,* Non-mHA, 6 weeks. NB is closely following the surface of the macropore. Bar = 50 µm. *D,* mHA, 6 weeks. Defect border where arrow denotes bone remodeling in MB. NB is observed inside pores of the scaffold. Bone has established contact with the outer surface of the scaffold and the inner surface of the macropore. Bar = 400 µm. *E,* mHA, 6 weeks. Macropore inside scaffold lined and filled by NB. Bar = 50 µm. *F,* mHA, 6 weeks. NB is closely lining the surface inside the macropore. Bar = 50 µm.

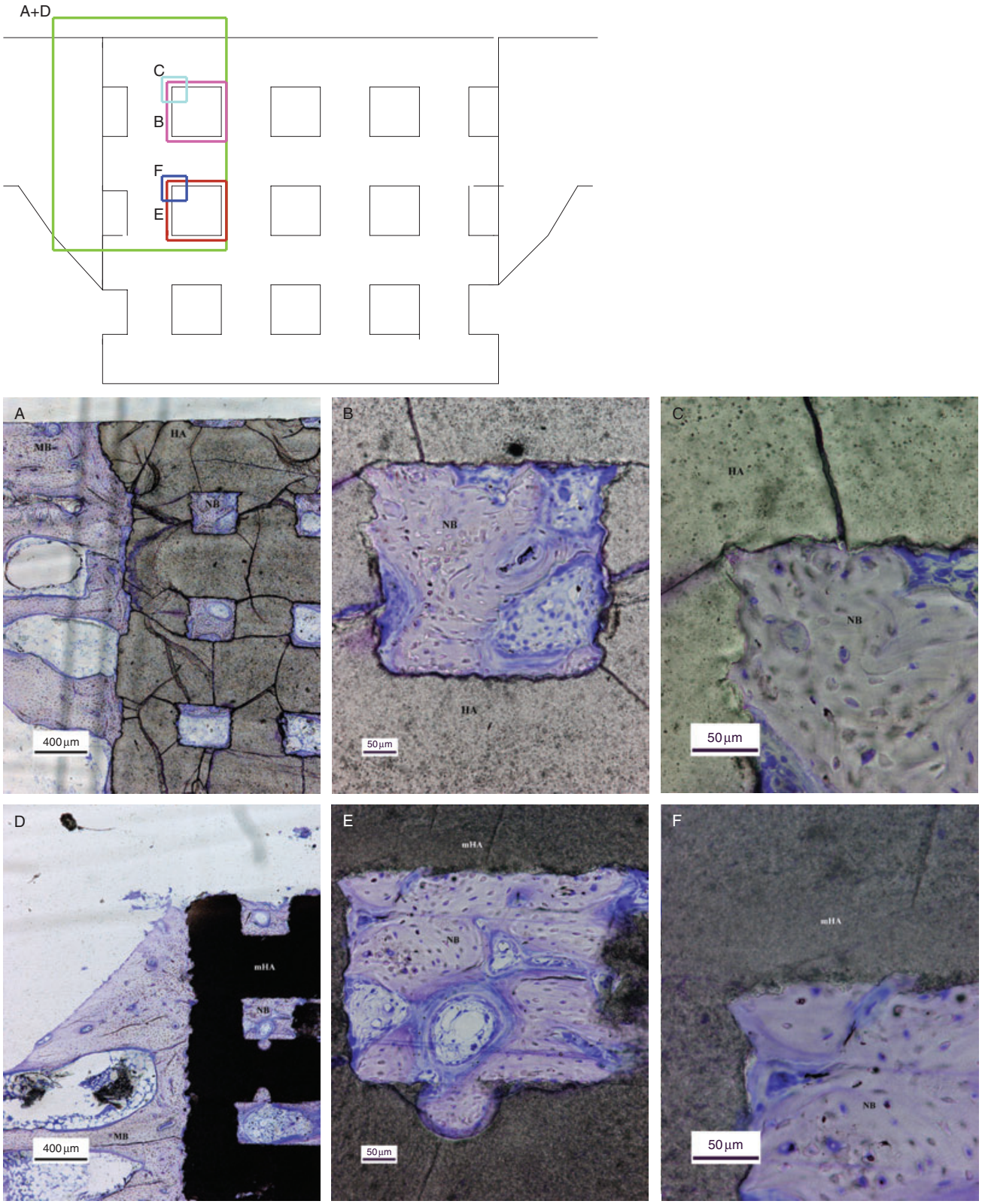

Figure 5A–F Mount of light micrographs (ground sections) of scaffolds in femur located according to schematic picture (insert, top). *A,* Non-microporous hydroxyapatite (mHA), 6 weeks. Defect border of mature bone (MB) undergoing remodeling. Newly formed bone (NB) in the defect border is reaching into the macropore and has established contact with the surface of the scaffold. Cracks in hydroxyapatite (HA) are caused by histological preparation. Bar = 400 µm. *B,* Non-mHA, 6 weeks. Macropore inside scaffold being filled with NB. Bar = 50 µm. *C,* Non-mHA, 6 weeks. NB is lining and filling the inner pore volume. Bar = 50 µm. *D,* mHA, 6 weeks. Defect border consisting of MB and NB. The NB is reaching the surface of the mHA scaffold. Bar = 400 µm. *E,* mHA, 6 weeks. The luminal surface of a macropore inside the scaffold has a lining of NB and the main portion is filled with NB. Bar = 50 µm. *F,* mHA, 6 weeks. NB in close contact with the surface of the macropore. Bar = 50 µm.

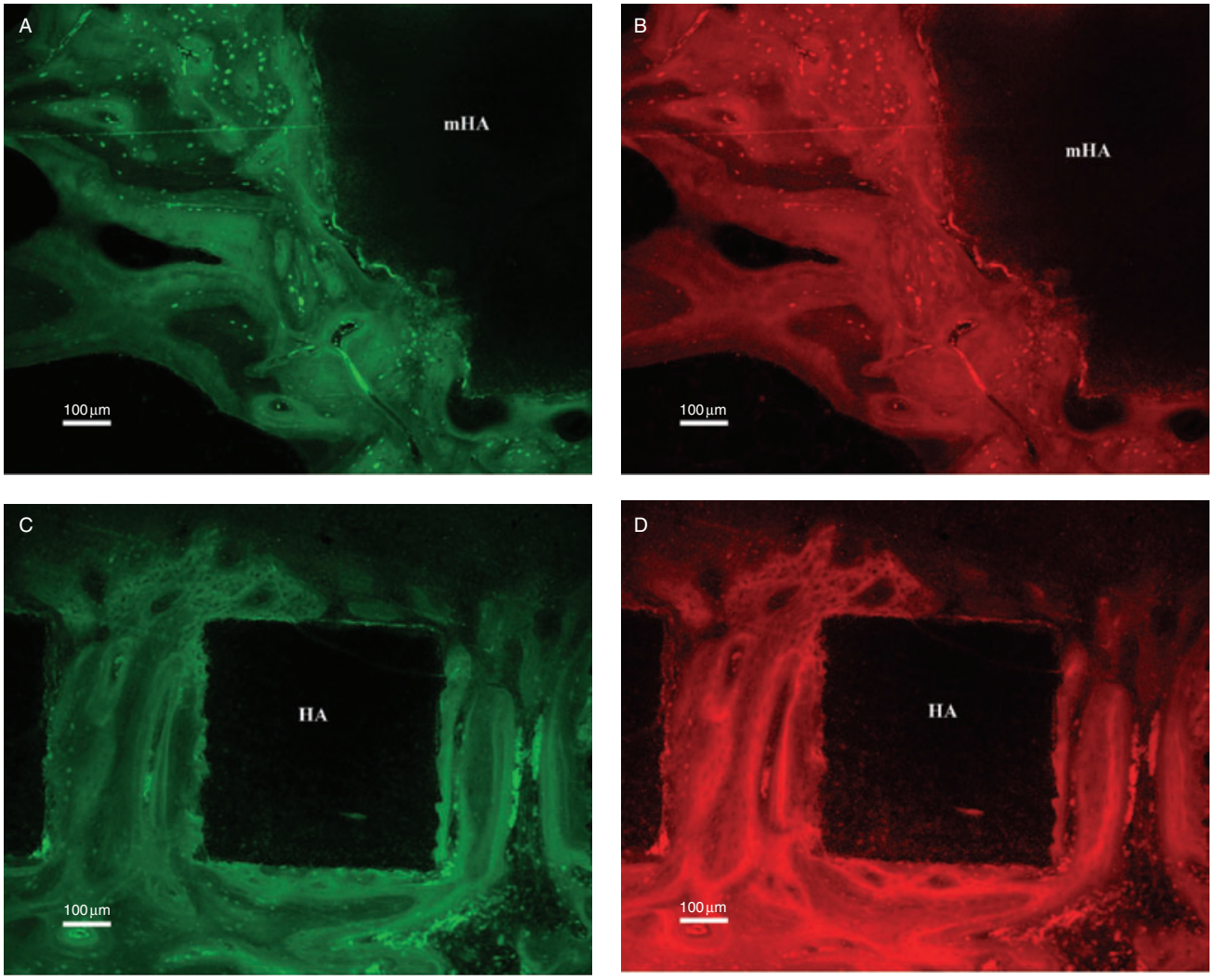

Figure 6A–D Mount of fluoroscopical micrographs (ground sections) of scaffolds in tibia and femur. *A + B,* Microporous hydroxyapatite (mHA) in femur. The presence of lines of oxytetracycline (A) and alizarin red (B) given 4 and 5 weeks postoperatively indicates that the bone has been formed and remodeled at 4 weeks. Bar = 100 µm. *C + D,* Non-mHA in tibia. The presence of lines of oxytetracycline (A) and alizarin red (B) given 4 and 5 weeks postoperatively indicates that the bone has been formed and remodeled at 4 weeks. Bar = 100 µm.

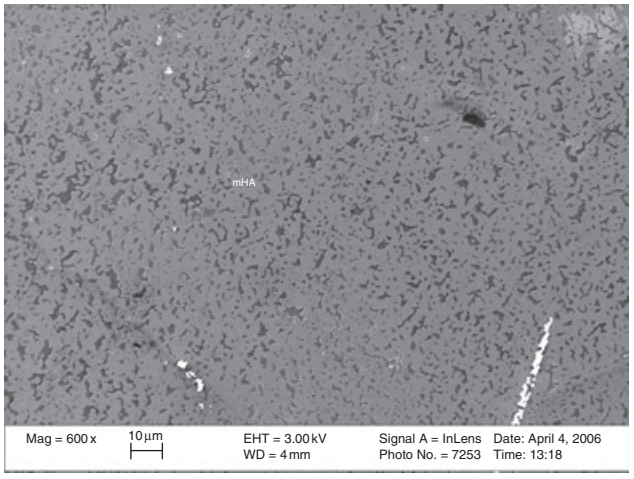

Figure 7 Surface of microporous hydroxyapatite. Bar = 10 µm.

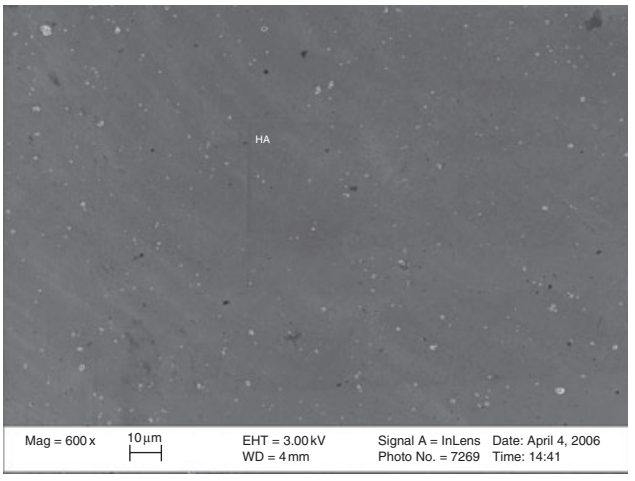

Figure 8 Surface of non-microporous hydroxyapatite. Bar = 10 µm.

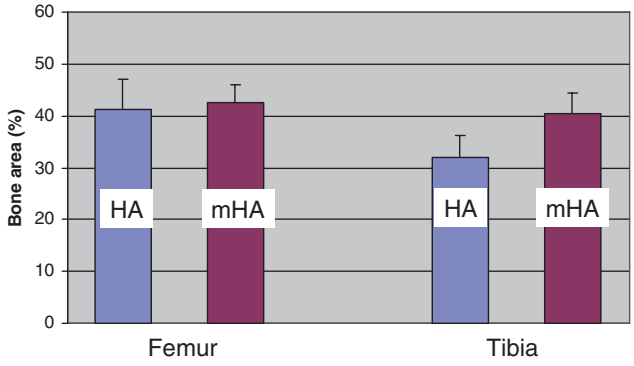

Figure 9 Results from bone area measurements presented for femoral and tibial sites. Non-microporous hydroxyapatite (mHA), mHA.

differentiate into the osteogenic lineage. Even if recent in vitro and in vivo studies have tried to demonstrate positive effects by adding microporosity to ceramics in bone,[15,16] there have been reports that the addition of 3 to 29 vol.% microporosity to HA cylinders does not affect neither osseointegration nor osseoconductivity when implanted in rabbit femur for 8 to 12 weeks.[13] Considering studies dealing with microporous ceramics, it is difficult to compare when design, material chemistry, and processing techniques vary.[5,11,13] As when describing macropores in ceramic scaffolds, it is therefore important that the compared microporosity is also being well defined. The use of designed scaffolds makes it possible to evaluate bone response in scaffolds with and without microporosity in a reliable manner. The addition of microporosity was, in this study, seen to promote the larger bone area/contact compared to an identical macroporous scaffold. Further analyses are needed to unravel the mechanisms by which chemistry and microporosity promote bone response in designed ceramic scaffolds. As suggested by the present observations, it is possible to further enhance the bone response by the addition of microporosity.

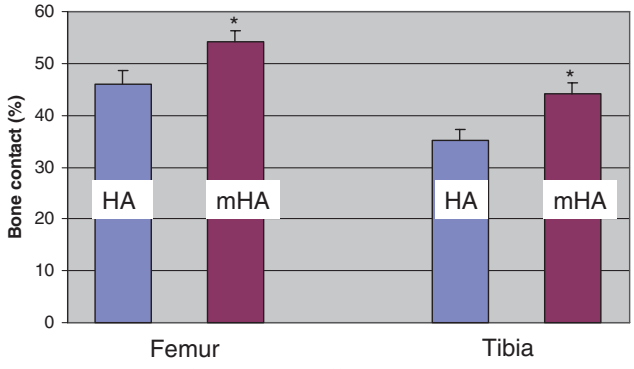

Figure 10 Results from bone-scaffold contact measurements presented for femoral and tibial sites. Non-microporous hydroxyapatite (mHA), mHA. *$p < .05$ in comparison with non-mHA.

CONCLUSIONS

Scaffolds of HA with identical macroporosity have been produced using an FFF technique – with and without microporosity. Using LM histomorphometry, more bone ingrowth and bone contact were detected inside the mHA scaffolds.

ACKNOWLEDGMENTS

This study was supported by the VINNOVA VinnVäxt Program, Biomedical Development in Western Sweden, Institute for Biomaterials and Cell Therapy, the Swedish Research Council (grant K2006-73X-09495-16-3), and the Hjalmar Svensson Foundation. We thank Lena Emanuelsson, Dr. Tobias Jarmar, and Dr. Magnus Hakeberg.

REFERENCES

1. Klawitter JJ, Hulbert SF. Application of porous ceramics for the attachment of load bearing internal orthopedic applications. J Biomed Mater Res 1971; 5:161–229.
2. Jarcho M. Calcium phosphate ceramics as hard tissue prosthetics. Clin Orthop 1981; 157:259–278.
3. Klein CP, de Groot K, van Kamp G. Activation of complement C3 by different calcium phosphate powders. Biomaterials 1983; 4:181–184.
4. Okumura M, Ohgushi H, Dohi Y, et al. Osteoblastic phenotype expression on the surface of hydroxyapatite ceramics. J Biomed Mater Res 1997; 37:122–129.
5. Hing KA, Annaz B, Saeed S, Rerell PA, Buckland T. Microporosity enhances bioactivity of synthetic bone graft substitutes. J Mater Sci Mater Med 2005; 16:467–475.
6. Uchida A, Nade S, McCartney E, Ching W. Bone ingrowth into three different porous ceramics implanted into the tibia of rats and rabbits. J Orthop Res 1985; 3:65–77.
7. Schliephake H, Neukam FW, Klosa D. Influence of pore dimensions on bone ingrowth into porous hydroxyapatite blocks used as bone graft substitutes. A histometric study. Int J Oral Maxillofac Surg 1991; 20:53–58.
8. Shimazaki K, Mooney V. Comparative study of porous hydroxyapatite and tricalcium phosphate as bone substitute. J Orthop Res 1985; 3:301–310.
9. Eggli PS, Muller W, Schenk RK. Porous hydroxyapatite and tricalcium phosphate cylinders with two different pore size ranges implanted in the cancellous bone of rabbits. A comparative histomorphometric and histologic study of bony

ingrowth and implant substitution. Clin Orthop 1988; 232:127–138.
10. Le Huec JC, Schaeverbeke T, Clement D, Faber J, Le Rebeller A. Influence of porosity on the mechanical resistance of hydroxyapatite ceramics under compressive stress. Biomaterials 1995; 16:113–118.
11. Bignon A, Chouteau J, Chevalier J, et al. Effect of micro- and macroporosity of bone substitutes on their mechanical properties and cellular response. J Mater Sci Mater Med 2003; 14:1089–1097.
12. Habibovic P, Yuan H, van der Valk CM, et al. 3D microenvironment as essential element for osteoinduction by biomaterials. Biomaterials 2005; 26:3565–3575.
13. Rosa AL, Beloti MM, Oliveira PT. Osseointegration and osseoconductivity of hydroxyapatite of different microporosities. J Mater Sci Mater Med 2002; 13:1071–1075.
14. Rosa AL, Beloti MM, van Noort R. Osteoblastic differentiation of cultured rat bone marrow cells on hydroxyapatite with different surface topography. Dent Mater 2003; 19:768–772.
15. Hing KA, Saeed S, Buckland T, Rerell PA. Microporosity affects bioactivity of macroporous hydroxyapatite bone graft substitutes. Key Eng Materials 2004; 273–276.
16. Annaz B, Hing KA, Kayser M, Buckland T, Di Silvio L. Porosity variation in hydroxyapatite and osteoblast morphology: a scanning electron microscopy study. J Microsc 2004; 215:100–110.
17. Donath K. Die Trenn-Dunnscliff-Technik zur Herstellung histologischer Präparaten von nicht schneidbaren Geweben und Materialen. Der Präparator 1988; 34:318–325.
18. Donath K, Breuner G. A method for the study of undecalcified bones and teeth with attached soft tissues. The Sage-Schliff (sawing and grinding) technique. J Oral Pathol 1982; 11:318–326.
19. Bohner M, van Lenthe GH, Grunenfelder S, et al. Synthesis and characterization of porous beta-tricalcium phosphate blocks. Biomaterials 2005; 26:6099–6105.
20. Hing KA, Best SM, Bonfield W. Characterization of porous hydroxyapatite. J Mater Sci Mater Med 1999; 10:135–145.
21. Li S, De Wijn JR, Li J, Layrolle P, De Groot K. Macroporous biphasic calcium phosphate scaffold with high permeability/porosity ratio. Tissue Eng 2003; 9:535–548.
22. Simon JL, Roy TD, Parsons JR, et al. Engineered cellular response to scaffold architecture in a rabbit trephine defect. J Biomed Mater Res A 2003; 66:275–282.
23. Malmström J, Adolfsson E, Emanuelsson L, Thomsen P. Bone ingrowth in zirconia and hydroxyapatite scaffolds with identical macroporosity. J Mater Sci Mater Med 2007. (In press)
24. Sennerby L, Dasmah A, Larsson B, Iverhed M. Bone tissue responses to surface-modified zirconia implants: a histomorphometric and removal torque study in the rabbit. Clin Implant Dent Relat Res 2005; 7(Suppl 1):S13–20.
25. LeGeros RZ. Properties of osteoconductive biomaterials: calcium phosphates. Clin Orthop Relat Res 2002; 395:81–98.